Performance Enhancement of Cooperative MIMO-NOMA Systems Over Sub-6 GHz and mmWave Bands

Ahmed A. Saleh and Mohamad A. Ahmed

College of Electronics Engineering, Ninevah University, Mosul, Iraq

Abstract — In this paper, two radio links with different frequency bands are considered for base stations (BS) serving users via decode-and-forward (DF) cooperative relays. Backhaul and access links are proposed with sub-6 GHz and millimeter wave (mmWave) bands, respectively. Non-orthogonal multiple access (NOMA) is employed in the backhaul link to simultaneously transmit a superposed signal in the power domain, using the same band. The superposed signals, containing two signals that differ in terms of power allocation factors (PAFs), are designed for two selected DF relays in the BS. The two relays are chosen from several relays to be serviced by the BS based on a pairing algorithm that depends on different users' circumstances. The furthest DF relay detects the incoming NOMA signal directly, while the nearest one applies successive interference cancellation (SIC) before extracting its signal. Each DF relay forwards the detected signals toward their intended users over mmWave channels. Three performance metrics are utilized to evaluate the system's performance: outage probability, achievable throughput, and bit error rate. Comparisons between two mmWave bands in the access link (28 and 73 GHz) are made to demonstrate the superiority of the 28 GHz band in terms of the three performance-related metrics.

Keywords — error probability, MIMO, mmWave, NOMA, outage probability, power allocation factor, successive-interference cancellation (SIC).

1. Introduction and Related Work

As opposed to traditional orthogonal multiple access (OMA) schemes, the non-orthogonal multiple access (NOMA) approach encourages multiple users to transmit data simultaneously by utilizing the same code and over the same frequency, but with different power levels [1]. Users with better channel conditions are assigned with less power based on the NOMA theory, and by using successive interference cancellation (SIC) [2], they are able to decode the data and hence, are aware of the signals corresponding to other users. This feature can be used to improve performance, but it was not taken into account in previous versions of NOMA [3].

To effectively utilize the old information included in NOMA systems, a cooperative NOMA transmission scheme is presented in this paper. The sequential detection approach is used at the receivers in particular, since users with higher channel gain must detect and decode signals of other users with weak channel conditions, by using the SIC strategy at their terminals. The users with good channel conditions can be utilized as repeaters, i.e. relays, to enhance the reliability of the received signals of the users with weak channel gain. Messages are sent from users with better channel conditions to those with worse channel conditions by employing short-range local communication techniques, such as ultra-wideband (UWB) and Bluetooth.

The analytical outcomes show that the largest diversity gain for all users can be obtained via NOMA but due to the difficulty of coordinating user participation, requesting all users under the coverage of a NOMA network to be engaged may not be feasible in practice. Moreover, grouping users with high channel quality does not always result in a significant performance improvement over OMA. Therefore, the technique of user pairing can be a promising approach for minimizing system complexity [4]. Instead, it is preferred to connect users who have more distinct channel profiles, i.e. they show a significant difference in channel gains due to different distances and attenuation conditions [5].

Multiple-input multiple-output (MIMO) techniques have emerged as a key enabler for next-generation wireless communication systems due to their ability to enhance the spectral efficiency and reliability of wireless links. MIMO-based non-orthogonal multiple access (MIMO-NOMA) is one of the promising techniques that have recently gained significant attention within the research community. MIMO-NOMA combines the benefits of MIMO with the concept of non-orthogonal multiple access (NOMA) to provide higher spectral efficiency and improved performance in downlink transmissions.

The huge demand for mobile multimedia services and for accessing data anytime and anywhere has forced telecommunications companies to reconsider how cellular networks are built. Wireless businesses have developed a new fifth-generation (5G) standard to satisfy this demand. Over the past few years, interest in research on next-generation 5G wireless systems which aspire to address multiple unprecedented technical requirements and obstacles, has grown in both academia and industry.

It is possible to consider increasing energy- and spectrum-related efficiency of the widely used 4G network, with

0.6–3 GHz bands being essentially congested, to satisfy the 5G criteria. Studies indicate that this gain will not be sufficient to offer the capacity required of 5G networks. Due to the vast amount of accessible bandwidth, mmWave frequency ranges between 30 and 300 GHz have drawn a lot of attention regarding addressing the capacity requirements of 5G networks. Although mmWave frequencies have a very wide range of usable bandwidth [6], their propagation properties differ greatly compared to sub-6 GHz and microwave bands. Theoretically, mmWave frequencies range from 30 GHz upwards. However, "mmWave bands" is a name given by wireless researchers to frequency ranges exceeding 6 GHz [7], [8].

Cooperative communication performance has been investigated for various relaying protocols, topologies, and system parameters. It has been specifically determined how well amplify-and-forward (AF) and decode-and-forward (DF) relay networks perform – for various fading channels – in terms of capacity, diversity gain, outage probability, and BER [9]. To estimate the transmitted signals in networks with several relays, the destination must first combine the received signals. The maximum signals received from many routes have regularly been split using ratio combining (MRC).

The digital beamforming (DB) technique can be employed by equipping each antenna with one radio frequency chain in order to take full advantage of MIMO. Since earlier and contemporary wireless systems have a few antennas only, DB is a viable design strategy for these systems (approx. 10) [10]. It is not possible to dedicate separate RF chains to each antenna, because mmWave systems are often equipped with massive antenna arrays. This inspires designers to develop a system that employs a MIMO mmWave band in which one RF chain can be used for multiple antennas, i.e. the number of RF chains is significantly lower than the number of utilized antennas. The combination of analog and digital beamforming, known as hybrid beamforming, is considered to be one of the most efficient methods for reducing RF chain for the entire MIMO system.

The ability of MIMO systems to send separate information via various antenna elements is also well-known (spatial multiplexing). In particular, mmWave systems are suitable for the deployment of many (between 100 and 1,000) antennas. Additionally, these aerials are designed to work in uncongested bands with very high frequencies, with the available bandwidths reaching tremendously high values. For example, at 60 GHz the bandwidth can be even 7 GHz. Therefore, multiplexed transmissions relying on spatial techniques over mmWave bands are encouraged, as they significantly improve overall system performance [11]. By employing this kind of multiplexing, the outgoing stream of the signals is divided into many portions, each of which is delivered in parallel, over the same RF chain associated with various antennas. This multiplexing gain boosts transmission throughput. Additionally, in order for transmissions relying on this technique to be successful, the channel needs to offer suitable inter-space between the antennas that are positioned close together. Applying appropriate inter-space between the antennas for a single-user system and the directivity of the information for

a multiuser system, respectively, are factors that may enable spatial multiplexing [12].

Mobile edge computing (MEC) utilizing the MIMO-NOMA approach has been proposed in [13] to cope with the high demand for suitable data rates observed in sixth generation wireless communication networks (6G). In the paper, the transmission delay existing in a MEC-MIMO-NOMA system was minimized for the sake of enhancing spectral and energy efficiencies. Moreover, the hybrid MEC-MIMO-NOMA analysis has been applied for the purposes of the aforementioned minimization, using generalized singular-value decomposition (SVD) and Dinkelbach transform. In this context, ergodic capacity available over a different number of antennas in the transmitter and receiver has been analyzed and compared as well in [14]. Frequency non-selective flat Rayleigh fading channels have been considered, demonstrating a linear proportion of the ergodic capacity and the number of antennas.

Besides, maximization of the secrecy sum rate for NOMA-MIMO in the uplink mode has been introduced in [15] by utilizing generalized SVD. The study took into account the constraints of obtaining a higher quality of service (QoS) and the maximum transmitted power.

The main contributions of this paper are related to a cooperative system that consists of a base station (BS) that provides services to users via decode-and-forward (DF) relays over the MIMO-NOMA mechanism. This helps enhance the end-to-end (E2E) performance in terms of capacity, error probability, and outage probability. This is because MIMO DF relay nodes are capable of transmitting over two different bands (sub-6 GHz and mmWave). The latter, which is considered to be an uncongested frequency band at the time of writing this paper, has different carrier frequencies with numerous wide bandwidths compared to other sub-6 GHz bands. Furthermore, MIMO-NOMA with these DF relays is capable of significantly enhancing spectral efficiency and exploiting the available transmitted power, with less dispersion.

The mechanism of the proposed system begins by applying a pairing algorithm, in which two relays are selected depending on the locations of all relays in the area of coverage, and according to the required rates of the users connected to the relays. Moreover, two links are used to deliver the signals to the end users, in which sub-6 GHz and mmWave bands are used for backhaul and access links, respectively. All terminals in the proposed network are equipped with multiple antennas to implement this transmission.

The NOMA technique is applied in the backhaul sub-6 GHz link, by serving the two selected DF relays in the power domain, i.e. simultaneously superposing two signals with different power allocation factors over the same selected frequency band. The DF relays complete signal processing by applying equalization, interference cancellation, signal decoding, re-encoding, and re-transmitting over mmWave bands of either 28 GHz or 73 GHz. Mathematical expressions of the entire system, related to its two hops, are derived to follow the signal processing and the modeling of all channels. Error and

outage probabilities, along with the achievable capacity, are evaluated to demonstrate the system's performance. A significant comparison between the two mmWave modes mentioned above is provided over a different number of MIMO antennas and transmitted power ratings.

2. System Modeling

Without loss of generality, we propose a pairing algorithm that couples an even number of relays (i.e. $2K$) into K pairs (Algorithm 1). It is applied by the base station (BS) after collecting the required channel state information (CSI) from all BS to relay channels, in addition to the intended rate for each user connected to a relay within the coverage area. We assume that the BS is equipped with N_{tx} and N_{rx} antennas for transmitting and receiving simultaneously. The PAFs are evaluated for each relay in the created pair, depending on the rate required by the user of interest related to that link.

Algorithm 1. Paring for NOMA relays with PAF evaluation.

Input← all BS-relay channel gains $\{H_1, H_2, \ldots, , H_{2K}\}$, number of groups K, number of relays $2K$, and number of users $2K$.

Input← The target rates for all users that are connected to the relays $\{r_1, r_2, \ldots, r_{2K}\}$.

1) The gains of BS-relay channels are sorted in descending order, i.e. $\|H_1\|_F^2 \geqslant \|H_2\|_F^2 \geqslant \ldots \geqslant \|H_{2K}\|\}_F^2$ in which the first half contains the channels of relays with higher channel gains, and the second half would be for relays the lower channel gains, i.e.

   $\{\|H_1\|_F^2, \|H_2\|_F^2 \ldots, \|H_K\|_F^2, \|H_{K+1}\|_F^2,$
   $\ldots, \|H_{2K}\|_F^2\}$.

2) Do pairing of the first relay in the first half, i.e. relay with channel H_1 with the first relays of the second half with channel H_{K+1}.

3) Remove the paired relays from the list, and repeat step 2 until all relays are paired into K groups.

4) According to the given target rates of all users, evaluate the PAFs for the paired relays by giving the user with a lower channel gain a higher PAF, while the other user would have the rest of the power.

5) Repeat step 4 for all pairs.

6) Examine the achieved rates for all users and calculate the gap between the obtained and the required rate.

7) If the gap is less than the threshold level, modify the PAF inside the pair itself, else substitute this user with a user in another pair that has a gap with a positive value, i.e. perform rate greater than its required rate.

Output: Set of pairs with the optimum PAF for each user.

After applying this algorithm, we focus on analyzing and evaluating the performance of one pair that contains two DF-relays, in which the BS provides NOMA services over

sub-6 GHz channels, and each relay delivers the BS services to the intended user with a required rate.
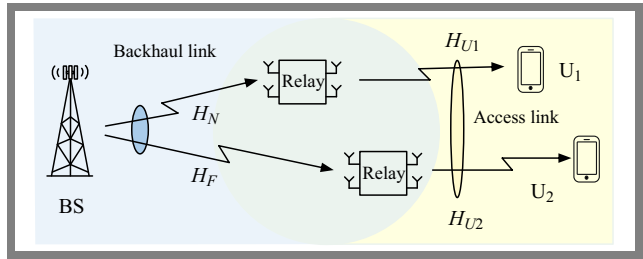

Fig. 1. Backhaul and access links via DF relays.

Such a system is shown in Fig. 1, where all nodes are supplied with multiple antennas for their transmissions, i.e. the system operates in the MIMO mode. The BS transmits the signal over a non-selective Rayleigh fading channel, to the decode-and-forward (DF) relay in the backhaul link, where the relay decodes and retransmits it over the mmWave channel to the terminal user. The two links work with different frequencies, with the backhaul link relying on the sub-6 GHz band, while the access link operates based on the mmWave band at 28 or 73 GHz.

2.1. First Hop from BS to Relay (Backhaul Link)

Figure 2 illustrates how the BS interacts with two relays which simultaneously use the same frequency resources while relying on power domain multiplexing. By assigning power to each relay according to its distance from the source, superposition coding is accomplished. When employing the PAF technique, the higher ratio of the available power is supplied to the furthest relay, and the remaining power is allocated to the closest relay. Nevertheless, the sum of this factors for all relays must be equal to one. Since more power is allocated to the far relay, the superposed power of the near relay is considered additive noise. Therefore, direct detection is used at the far relay without the need to perform SIC.
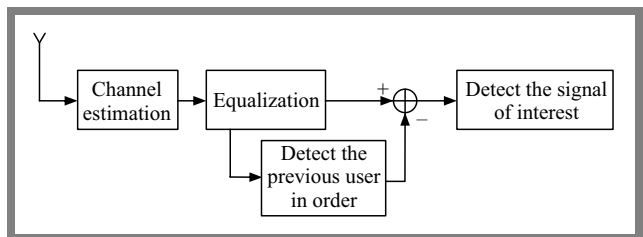

Fig. 2. SIC process performed by the near relay to form the superposed NOMA received signal [16].

On the other hand, at the near relay terminal, the SIC process must be applied. This process includes detecting the signal of the far relay which is then subtracted from the entire NOMA signal received in order to construct the near relay's signal. Algorithm 2 and Fig. 2 explain and show the SIC process in detail. We assume flat Rayleigh fading channels, i.e. frequency non-selective channels, for the first hop. The modulated signals for the far and near relays are denoted by x_f and x_n, respectively, and the quadrature phase shift keying (QPSK) modulation scheme is used for all links.

Algorithm 2. SIC at the near user terminal.

Input: $\boldsymbol{H}_N$ and $\boldsymbol{Y}_N$

1) Apply ZF equalization to remove the effect of channel $\boldsymbol{H}_N$, i.e. $\overline{\boldsymbol{x}}_{NOMA} = \frac{\boldsymbol{Y}_N}{\boldsymbol{H}_N} = \boldsymbol{x}_{NOMA} + \frac{\boldsymbol{w}_N}{\boldsymbol{H}_N}$.

2) From $\overline{\boldsymbol{x}}_{NOMA}$ $\boldsymbol{x}_F$ is detected directly, since it has a higher superposed power value.

3) Convolve the detected $\boldsymbol{x}_F$ with $\boldsymbol{H}_N$ to create the far user signal over the near user channel, i.e. $\boldsymbol{H}_N\boldsymbol{x}_F$.

4) $\boldsymbol{H}_N\boldsymbol{x}_F$ is subtracted from the entire received NOMA signal, i.e. $\boldsymbol{Y}_N - \boldsymbol{H}_N\boldsymbol{x}_F$ for the construction of the near relay's signal with a level of inherent noise, i.e. $\boldsymbol{H}_N\boldsymbol{x}_N + \boldsymbol{w}_N$.

5) Apply equalization to the signal obtained in step 4, i.e. $\overline{\boldsymbol{x}}_N = \boldsymbol{x}_N + \frac{\boldsymbol{w}_N}{\boldsymbol{H}_N}$.

6) The noisy version of the near symbol user $\overline{\boldsymbol{x}}_N$ is then obtained and converted to bits depending on the modulation scheme already used at the BS.

7) Interference-free near-user signal $\overline{\boldsymbol{x}}_N$.

Output: Set of pairs with the optimum PAF for each user.

The BS employs a pairing algorithm for the sake of choosing two relays from several which are present within the coverage area. The NOMA technique is applied on those two paired relays, where each DF relay receives, decodes, and retransmits its incoming signal to a user in the access link via a mmWave channel. PAF is applied at the BS for those two relays, the far and near relays are allocated with power levels of $\alpha_F p_t$ and $\alpha_N p_t$, where $\alpha_F + \alpha_N = 1$ and $\alpha_F > \alpha_N$. Additionally, at the BS, the NOMA signal is created by superposing the two signals that allocated the suitable PAF for each of them. This process can be expressed as:

$$\boldsymbol{x}_{NOMA} = \sum_{i=1}^{N_U} \sqrt{p_t \alpha_i \boldsymbol{x}_i} \,, \tag{1}$$

where N_U represents the number of users. However, here, for two users, we assume that near and far users are identified with N and F symbols, respectively.

The signals received at the two relays are defined as Y_f and Y_n and can be written as:

$$\boldsymbol{Y}_i = \boldsymbol{H}_i \boldsymbol{x}_{NOMA} + w_i \,, \quad i \in \{F, N\} \,, \tag{2}$$

in which $\boldsymbol{H}_F$ and $\boldsymbol{H}_N$ are the channels for far and near relays, respectively, with $\|\boldsymbol{H}_F\|_F^2 < \|\boldsymbol{H}_N\|_F^2$, where $\|\boldsymbol{A}\|_F$ represents the Frobenius normalization of matrix $\boldsymbol{A}$. It is noteworthy that $\|\boldsymbol{H}\|_F^2 = \text{trace}(H \times H^H)$ is exploited to measure the channel gain. In more detail, this process is obtained as:

$$\|H\|_F^2 = \text{trace}(H \times H^H)$$
$$= \sum_{n=1}^{N_{rx}} \sum_{m=1}^{N_{tx}} |H(n,m)|^2 = \sum_{k=1}^{n} |\lambda_k|^2 \,, \tag{3}$$

in which λ_k is the eigenvalues associated with the eigenvectors of the MIMO channel matrix. An alternative method is detailed in [13]–[15] and relies on using generalized singu-

lar value decomposition (GSVD) – a technique considered to be an efficient approach to channel evaluation. It is worth noting that the two methods can be applied to any number of transmitting and receiving antennas, i.e. to squared and non-squared channels.

Furthermore, $w_F \sim CN(0, \sigma_{w_F}^2)$ and $w_N \sim CN(0, \sigma_{w_N}^2)$ are the additive white Gaussian noise at the far and near relay terminals with zero mean and variance of $\sigma_{w_F}^2$ and $\sigma_{w_N}^2$, respectively. The DF relays process the received NOMA signals, whereas the far relay directly detects the incoming signal by applying SIC. This detection starts with equalizing the channel by using zero-forcing (ZF) equalization, and then continues with detecting the transmitted symbols $\boldsymbol{x}_F$. These symbols are transmitted to the second user equipment U_2, via a mmWave channel.

For the near relay, the SIC process is compulsory in order to construct the signal from the entire incoming NOMA signal, as explained in Algorithm 1. After applying SIC, the detected symbols of the near relay are forwarded to the first user U_1. At the far relay, the throughput can be evaluated as:

$$R_F = \log_2(1 + \gamma_F) \,, \tag{4}$$

where γ_F is the signal-to-interference-plus-noise ratio (SINR) at the far-relay and is expressed as:

$$\gamma_F = \frac{p_t \alpha_F \|\boldsymbol{H_F}\|_F^2}{p_t \alpha_N \|\boldsymbol{H_F}\|_F^2 + \sigma_{w_F}^2} \,. \tag{5}$$

The throughput at the near relay terminal is:

$$R_n = \log_2(1 + \Omega_N) \,, \tag{6}$$

where Ω_N is the signal-to-noise ratio (SNR) at the near relay after applying SIC and after removing the far relay's signal. The SNR (Ω_N) is:

$$\Omega_N = \frac{p_t \alpha_n \|\boldsymbol{H_N}\|_F^2}{\sigma_{w_N}^2} \,. \tag{7}$$

2.2. Second Hop from Relay to UE (Access Link)

Transmission over mmWave is another promising technology that has recently gained significant attention within the wireless communication community due to its potential to provide high data rates and large bandwidth. There are several types of large-scale path losses analyzed in this study, as shown in Tab. 1.

Tab. 1. Path loss exponent (PLE) for different environment scenarios [17].

Environment scenario	PLE
Free space	2
Urban area	2.7–3.5
Suburban area	3–5
Line of sight for indoor	1.6–1.8

We employ close-in (CI) free-space (FS) reference distance d_0 for the path loss (PL) model of 28 GHz and 73 GHz bands. The equation for the CI model is given by [18] as:

$$\text{PL [dB]} = \text{FSPL}(d_0) + 10n \log_{10}\left(\frac{d}{d_0}\right) + X_\sigma , \qquad (8)$$

where n is the minimum mean squared error (MMSE) optimum fit path-loss exponent (PLE), with specifically measured values for LoS and NLoS. Hence, it differs from frequency to frequency within the mmWave band. The shadow factor is denoted as X_σ and is represented by a Gaussian distribution random variable with a zero-mean and standard deviation of σ in dB. The distance between the transmitter and the receiver is denoted by d in Eq. (8). All these factors are presented in Tab. 2 for the all frequencies used and for the measurements achieved in [18], [19] over antennas at the transmitter and receiver with isotropic gains defined in dBi as G_{tx} and G_{rx}, respectively.

Tab. 2. Summarized PLE (n) and standard deviations (σ) of the shadowing factor (X_σ) for the 28 GHz and 73 GHz frequencies at $d_0 = 1$ m [14], [15].

Frequency [GHz]	G_{tx}/G_{rx} [dBi]	LOS		NLOS	
		n	X_σ [dB]	n	X_σ [dB]
28 GHz	24.5/24.5	1.9	1.1	4.57	10.0
73 GHz	27/27	2.4	6.3	4.7	12.7

DF relays decode the signals after they have been received from the source and send the decoded signals to their destinations after changing the carrier to mmWave frequencies. To prevent error propagation, the relay successfully decodes estimates before sending them to the destination [20].

After extracting the signal of the intended user from the incoming NOMA signal at the near and far relays, the relays forward the decoded signals to U_1 and U_2. At each user terminal the received signal can be expressed as:

$$y_{U_k} = \boldsymbol{H}_{U_k} X_k + w_{U_k} \qquad k \in \{1, 2\} , \qquad (9)$$

where $w_{U_k} \sim CN(0, \sigma^2_{w_{U_k}})$ for $i \in \{1, 2\}$ denotes the AWGN at each user terminal. As the access hops are achieved via conventional orthogonal multiple access OMA, the capacity of this link for the two users can be evaluated as:

$$R_{U_k} = \frac{1}{2} \log_2\left(1 + \frac{p_t \left\| H_k \right\|^2_F}{\sigma^2_{w_{U_k}}}\right) \qquad k \in \{1, 2\} , \qquad (10)$$

in which the rate of 0.5 is related to the bandwidth being used twice for the OMA access link, while for the NOMA system in the backhaul link, this factor was equal to 1, since half of the bandwidth is exploited compared to OMA.

The end-to-end (E2E) rates for the two links at the two users' terminals are:

$$R_{T_1} = \min(R_F, R_{U_1}) ,$$
$$R_{T_2} = \min(R_N, R_{U_2}) , \qquad (11)$$

in which the lower capacity for any link would be dominant for that link. Furthermore, the achievable sum rate R_T, which is achieved by the BS, can be evaluated as:

$$R_T = E\left\{ R_{T_1} + R_{T_2} \right\} , \qquad (12)$$

where $E\{.\}$ denotes the expectation process which represents the mean of the achievable throughput of the two users.

3. Complexity Analysis

In this section, the arithmetic complexity of the proposed MIMO-NOMA scheme is evaluated. As mentioned earlier, each receiving terminal, i.e. the DF relay and the user's receiver, is required to apply a ZF equalizer to remove the effect of the channels. Moreover, it is required to apply SIC at all nodes operating with NOMA, except for the higher order node which is the furthest node from the service provider or the node that allocated with a larger portion of the available power. Thus, here we evaluate the number of operations required to accomplish the reception of the signal. Following the complexity analysis from [21], we can obtain the computational operations required to perform ZF and SIC at each relay. All nodes are equipped with N_{tx} transmitting antennas, N_{rx} receiving antennas, and each of the K DF relays is connected to a user. According to such parameters, the required number of matrix inversions is K, while the number of SIC operations is $K - 1$. The related mathematical complexity can be expressed as $\mathcal{O}(KN_{tx}N^3_{rx})$.

4. Simulation Results

In the simulation, two hops for involving signals traveling from a BS to two users are assumed, i.e. backhaul and access links. Multiple cases are considered to evaluate error probability, system capacity, and outage probability. Rayleigh fading channels are assumed for the sub-6 GHz backhaul link, i.e. the link from the BS to the relays, while mmWave frequency is considered in the access link between the relays and the users. Details about the two links are defined in Tab. 3.

Tab. 3. Simulation parameters and notations used.

Notation	Parameter	Value
f_a, BW	Operating frequency for access link bandwidth	28 GHz, 100 MHz and 73 GHz, 2000 MHz
f_b, BW	Operating frequency for backhaul link bandwidth	3.5 GHz, 25 MHz [22]
P_t	Transmitted power	0–50 dBm
N_0	Noise power	−174 dBm/Hz +10 log (BW)
$\alpha_1, \alpha_2 \in \{0, 1\}$	FAFs for the near and far relays, respectively	$\alpha_1 + \alpha_2 = 1$
Modulation scheme	QPSK	$\frac{1}{\sqrt{2}}(\pm 1 \pm \text{j}1)$

In the first hop, the relay associated with U_1 is assumed to be far from the BS. We assume the distance between them as $d_1 = 500$ m, and PAF is $\alpha_1 = 0.7$. The relay associated with

U_2 is assumed to be located near the BS, with the distance assumed as $d_2 = 300$ m, with PAF of $\alpha_2 = 0.3$. The access link between the DF relays and the users exploits the mmWave band (28 GHz or 73 GHz). In this link, we assumed, without the loss of generality, that the two users have the same distance from their corresponding relays, i.e. $d_3 = d_4 = 100$ m, and OMA is used in this link. It is noteworthy that the modulation scheme exploited in this paper is QPSK.

4.1. Backhaul Link and mmWave Access Link in the 28 GHz Band

In this scenario, a sub-6 GHz band of 3.5 GHz with a 25 MHz bandwidth is assumed to work with MIMO-NOMA in the backhaul link, i.e. the connection between the BS and the relays. The access link between the relays and the user exploits the mmWave mode of 28 GHz, with a 100 MHz bandwidth to transmit the detected data by the DF relays to the users with different transmitted power ratings. Figure 3 shows the throughput obtained by each user with the achievable sum-rate applied by the BS. We considered, in this simulation, that $N_{tx} = N_{rx} = 2$ for all terminals of the two hops.
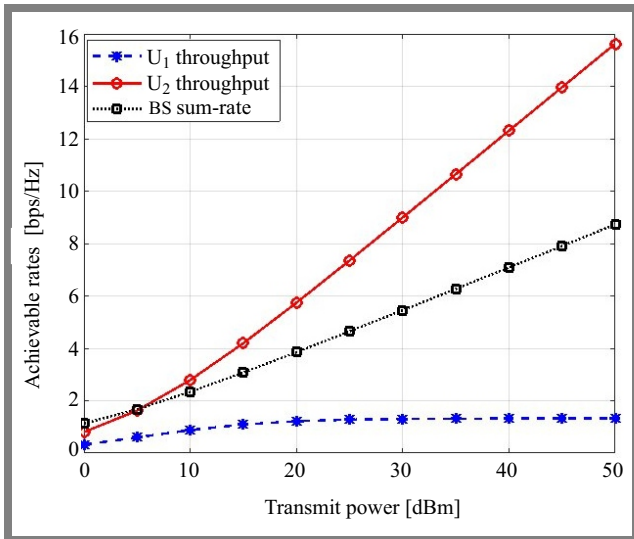

Fig. 3. E2E achievable capacity of two users with $d_1 = 500$ m, $d_2 = 300$ m, and $d_3 = d_4 = 100$ m, $N_{tx} = N_{rx} = 2$.

It is observed that the near user achieves better throughput than the far user because of employing SIC to remove the signal of the far user. The far user's throughput becomes saturated after approximately 25 dBm with 1.68 bps/Hz. The sum-rate achievable capacity is calculated by taking the mean of the sum of throughputs of the two users.

Figure 4 shows the outage probability of this scenario. It is the probability that the rate expressed in bps/Hz goes below the minimum threshold level required for a given user. It can be seen that U_1, which is connected to the near relay with a lower PAF of 0.3, has an outage probability that is approx. 5 dBm worse than the outage probability of U_2, which is connected to the far relay with a higher PAF of 0.7, when the target rates for the U_1 and U_2 are considered as $r_1 = 1$ bps/Hz and $r_2 = 3$ bps/Hz, respectively. A significant role is played by PAF in terms of optimizing the performance of the two users

and the entire system. This can be achieved by verifying this factor depending on the required rate of each node.
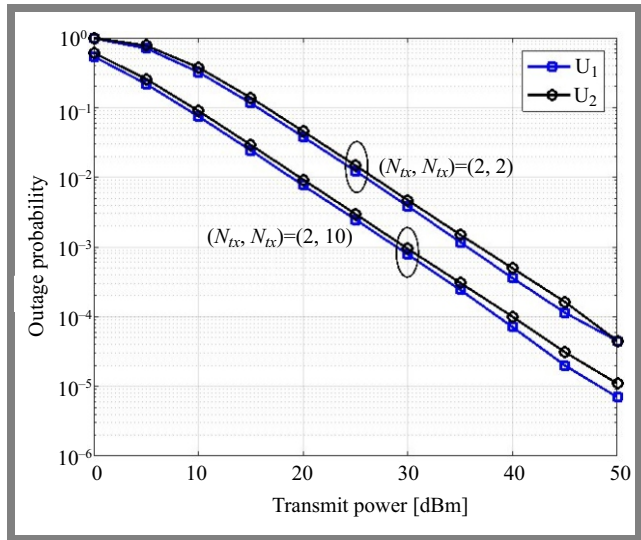

Fig. 4. Outage probability of two users with $d_1 = 500$ m, $d_2 = 300$ m, and $d_3 = d_4 = 100$ m, $(N_{tx}, N_{rx}) = (2, 2)$ and $(2, 10)$, the target rates are assumed as $r_1 = 1$ and $r_2 = 3$ bps/Hz.

The bit error rates (BER) over different transmitted powers are shown in Fig. 5. Two scenarios have been taken into account by changing the number of antennas in the receiver terminal of the relay and the user from 2 to 4, while fixing number of transmitting antennas at 2. It can be noticed from this figure that an increase in the number of receiving antennas offers an improvement by more than 25 dBm in this particular performance metric, at 10^{-4} BER.
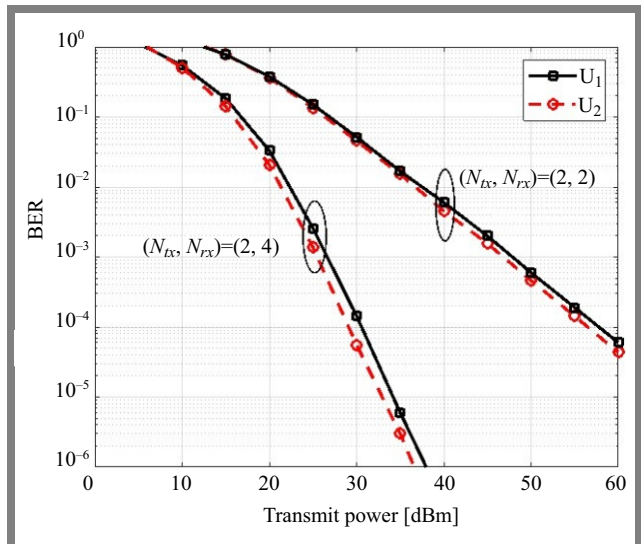

Fig. 5. E2E BER of two users over the 28 GHz access link, with $d_1 = 500$ m, $d_2 = 300$ m and $d_3 = d_4 = 100$ m, $(N_{tx}, N_{rx}) = (2, 2)$ and $(2, 4)$.

Figure 6 shows a three-dimensional plot of E2E throughput of the proposed system over different numbers of receiving antennas and with the transmitted power range P_t utilizing the 28 GHz band in the access link. It can be seen that an increase in the number of antennas in the receiving terminals

can significantly improve the throughput and such an increase in N_{rx} can satisfy throughput with a minimum P_t required. This plot also indicates the required power at a specific N_{rx} to achieve the intended throughput.
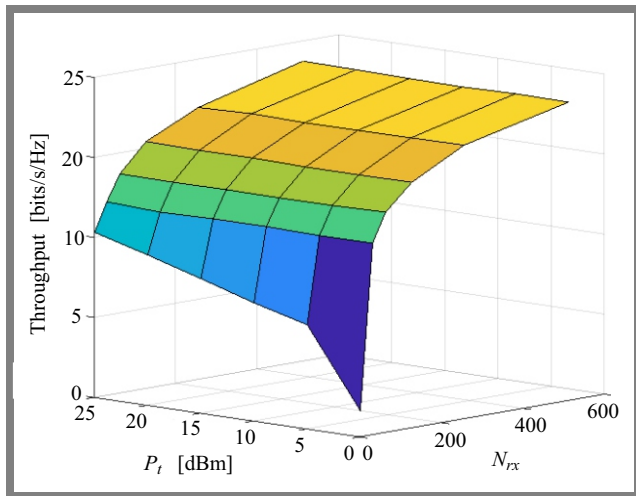

Fig. 6. E2E throughput for different numbers of receiver antennas at each terminal N_{rx} and for several values of transmitted power P_t.

4.2. Comparison of Access Links using 28 GHz and 73 GHz Bands

In the second part of the simulation results, we wish to compare two mmWave frequency bands of 28 GHz and 73 GHz. This can be achieved by changing the band in which the access link of the proposed system operates. Three performance metrics have been considered, i.e. achievable sum-rate of the BS, outage probability, and error probability (BER). In Fig. 7, the sum-rate produced by the BS is obtained for the two mmWave bands, with the throughput of the two users evaluated in the two hops taking the minimum ergodic capacity for each link, i.e. the minimum capacity at any link that would be dominant. Then, by evaluating the mean of the
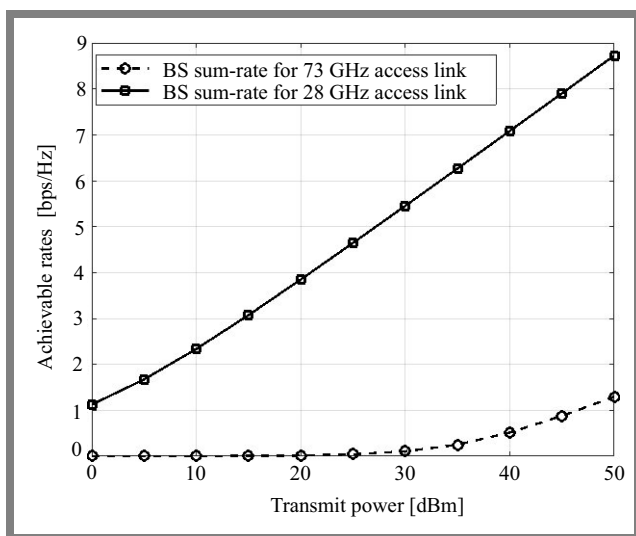

Fig. 7. BS sum-rate for the E2E system for 28 and 73 GHz access links, $d_1 = 500$ m, $d_2 = 300$ m and $d_3 = d_4 = 100$ m, $(N_{tx}, N_{rx}) = (2, 2)$.

summation of the two users' capacity, the achievable sum-rate of the BS is obtained. It can be seen that the 28 GHz band outperforms its 73 GHz counterpart in all transmitting power ranges, with more than 7 bps/Hz at $P_t = 50$ dBm. Here, the simple MIMO case of $(N_{tx}, N_{rx}) = (2, 2)$ has been considered.
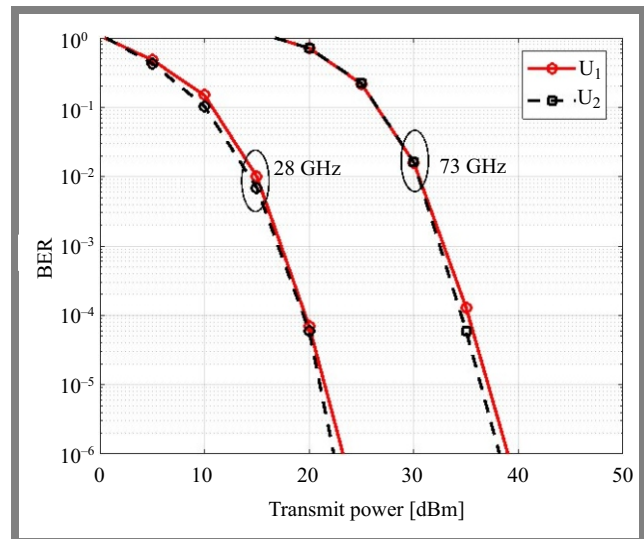

Fig. 8. BER comparison of two users with $d_1 = 500$ m, $d_2 = 300$ m and $d_3 = d_4 = 100$ m, $(N_{tx}, N_{rx}) = (2, 10)$, $\alpha_1 = 0.7$, $\alpha_2 = 0.3$.

Figure 8 shows E2E BER for those mmWave frequency bands that are used by the access link of the two users. In this simulation, we increase the number of antennas at each receiving terminal to 10 while keeping the number of transmitting antennas at 2, as it was the case before. Again, it can be seen that the band of 73 GHz needs about 15 dBm transmitting power from the BS to achieve the same BER at 10^{-5}.

5. Conclusion

In this paper, the process of rendering wireless communication services with the use a BS, DF relays and two links has been described. The first link is established between the BS and the DF relays. It is known as the backhaul link and relies on the sub-6 GHz mode, while the second link is established between the DF relays and the users. It is known as the access link and exploits the mmWave mode (28 GHz or 73 GHz). The MIMO-NOMA technique has been used in the backhaul link for a pair of relays that are chosen depending on the proposed pairing algorithm. The signals then have been delivered to the users after applying a full detection procedure in the DF relays, which may include SIC, depending on the value of PAF allocated to each relay. Achievable throughput, as well as error and outage probabilities have been evaluated for this system, with different scenarios taken into consideration. Comparisons between the two mmWave modes have been made, showing that the 28 GHz variety outperforms its 73 GHz counterpart due to higher attenuation. The results demonstrate the achievable rate that can be obtained over a different number of receiving antennas in all nodes, and

over a range of transmit power values generated by the BS. The findings may significantly assist in selecting the required number of receiving antennas for a particular transmit power rating, and vice versa.

References

[1] Y. Saito, A. Benjebbour, Y. Kishiyama, and T. Nakamura, "System-level performance evaluation of downlink non-orthogonal multiple access (NOMA)", *IEEE International Symposium on Personal, Indoor and Mobile Radio Communication PIMRC*, vol. 2, pp. 611–615, 2013 (https://doi.org/10.1109/PIMRC.2013.6666209).

[2] T.M. Cover and J.A. Thomas, *Elements of Information Theory*. Wiley, 748 p., 2005 (https://doi.org/10.1002/047174882X).

[3] J. Choi, "Non-orthogonal multiple access in downlink coordinated two-point systems", *IEEE Communication Letters*, vol. 18, no. 2, pp. 313–316, 2014 (https://doi.org/10.1109/LCOMM.2013.123113.132450).

[4] A.A. Saeed and M.A. Ahmed, "Cognitive radio based NOMA for the next generations of wireless communications", in *Proceeding of International Conference on Electronic, Engineering and Informatics*, vol. 2022, pp. 125–130, 2022 (https://doi.org/10.1109/ICELTICs56128.2022.9932105).

[5] Z. Ding, Z. Yang, P. Fan, and H.V. Poor, "On the performance of non-orthogonal multiple access in 5G systems with randomly deployed users", *IEEE Signal Processing Letters*, vol. 21, no. 12, pp. 1501–1505, 2014 (https://doi.org/10.1109/LSP.2014.2343971).

[6] T.E. Bogale and L.B. Le, "Massive MIMO and mmWave for 5G Wireless HetNet: Potential benefits and challenges", *IEEE Vehicular Technology Magazine*, vol. 11, no. 1, pp. 64–75, 2016 (https://doi.org/10.1109/MVT.2015.2496240).

[7] T.S. Rappaport *et al.*, "Wireless communications and applications above 100 GHz: Opportunities and challenges for 6G and beyond", *IEEE Access*, vol. 7, pp. 78729–78757, 2019 (https://doi.org/10.1109/ACCESS.2019.2921522).

[8] S. Sun *et al.*, "Propagation path loss models for 5G urban micro- and macro-cellular scenarios", *2016 IEEE 83rd Vehicular Technology Conference* (*VTC Spring*), China, pp. 1–6, 2016 (https://doi.org/10.1109/VTCSpring.2016.7504435).

[9] F. Gharari, T.M.C. Chu, and H.J. Zepernick, "Performance Analysis of a Piecewise-and-Forward Relay Network on Rayleigh Fading Channels", 2015 9th International Conference on Signal Processing and Communication Systems (ICSPCS), Australia, 2015. (https://doi.org/10.1109/ICSPCS.2015.7391753).

[10] D.P. Palomar, M.A. Lagunas, and J.M. Cioffi, "Optimum linear joint transmit-receive processing for MIMO channels with QoS constraints", *IEEE Transactions on Signal Processing*, vol. 52, no. 5, pp. 1179–1197, 2004 (https://doi.org/10.1109/TSP.2004.826164).

[11] D. Gesbert, H. Bölcskei, D.A. Gore, and A.J. Paulraj, "Outdoor MIMO wireless channels: Models and performance prediction", *IEEE Transaction on Communication*, vol. 50, no. 12, pp. 1926–1934, 2002 (https://doi.org/10.1109/TCOMM.2002.806555).

[12] T.E. Bogale, X. Wang, and L.B. Le, "mmWave communication enabling techniques for 5G wireless systems: A link level perspective", in *mmWave Massive MIMO: A Paradigm for 5G*, S. Mumtaz, L. Dai, and J. Rodriguez, Eds. Academic Press, pp. 195–225, 2017 (https://doi.org/10.1016/B978-0-12-804418-6.00009-1).

[13] Y. Dursun, F. Fang, and Z. Ding, "Hybrid NOMA based MIMO offloading for mobile edge computing in 6G networks", *China Communications*, vol. 19, no. 10. pp. 12–20, 2022 (https://doi.org/10.23919/JCC.2022.00.024).

[14] Y. Jia, P. Xu, and X. Guo, "MIMO system capacity based on different numbers of antennas", *Results in Engineering*, vol. 15, article no. 100577, 2022 (https://doi.org/10.1016/j.rineng.2022.100577).

[15] Y. Dursun, K. Wang, and Z. Ding, "Secrecy sum rate maximization for a MIMO-NOMA uplink transmission in 6G networks", *Physical Communication*, vol. 53, no. 11, article no. 101675, 2022 (https://doi.org/10.1016/j.phycom.2022.101675).

[16] M.A. Ahmed, A. Baz, and C.C. Tsimenidis, "Performance analysis of NOMA systems over Rayleigh fading channels with successive-interference cancellation", *IET Communications*, vol. 14, no. 6, pp. 1065–1072, 2020 (https://doi.org/10.1049/iet-com.2019.0504).

[17] T.S. Rappaport, K. Blankenship, and H. Xu, "Propagation and Radio System Design Issues in Mobile Radio Systems for the GloMo Project", (tutorial sponsored by DARPA), pp. 1–26, 1997.

[18] T.S. Rappaport, G.R. MacCartney, M.K. Samimi, and S. Sun, "Wideband millimeter-wave propagation measurements and channel models for future wireless communication system design", *IEEE Transactions on Communications*, vol. 63, no. 9, pp. 3029–3056, 2015 (https://doi.org/10.1109/TCOMM.2015.2434384).

[19] I.A. Hemadeh *et al.*, "Millimeter-wave communications: Physical channel models, design considerations, antenna constructions and link-budget", *IEEE Communications Surveys and Tutorials*, vol. 20, no. 2, pp. 870–913, 2017 (https://doi.org/10.1109/COMST.2017.2783541).

[20] J. He *et al.*, "A tutorial on lossy forwarding cooperative relaying", *IEEE Communications Surveys and Tutorials*, vol. 21, no. 1, pp. 66–87, 2019 (https://doi.org/10.1109/COMST.2018.2866711).

[21] E.N. Tominaga, O.L.A. Lopez, H. Alves, R.D. Souza, and J.L. Rebelatto, "Performance analysis of MIMO-NOMA iterative receivers for massive connectivity", *IEEE Access*, vol. 10, pp. 46808–46822, 2022 (https://doi.org/10.1109/ACCESS.2022.3170715).

[22] R. Verdecia-Peña and J.I. Alonso, "A two-hop mmWave MIMO NR-relay nodes to enhance the average system throughput and BER in outdoor-to-indoor environments", *Sensors*, vol. 21, no. 4, pp. 1–19, 2021 (https://doi.org/10.3390/s21041372).

———————

Ahmed A. Saleh
E-mail: ahmed.attallah2021@stu.uoninevah.edu.iq
College of Electronics Engineering, Ninevah University, Mosul, Iraq

Mohamad A. Ahmed, Ph.D.
Assistant Professor in Digital Communications
https://orcid.org/0000-0001-6412-2275
E-mail: mohamad.alhabbar@uoninevah.edu.iq
College of Electronics Engineering, Ninevah University, Mosul, Iraq